Effector selection precedes reach planning in the dorsal parietofrontal cortex

Pierre-Michel Bernier, Matthew Cieslak and Scott T. Grafton

J Neurophysiol 108:57-68, 2012. First published 28 March 2012;
doi: 10.1152/jn.00011.2012

J Neurophysiol 108: 57–68, 2012.
First published March 28, 2012; doi:10.1152/jn.00011.2012.

Effector selection precedes reach planning in the dorsal parietofrontal cortex

Pierre-Michel Bernier,[1] Matthew Cieslak,[2] and Scott T. Grafton[2]

[1]*Département de Kinanthropologie, Université de Sherbrooke, Sherbrooke, Quebec, Canada; and* [2]*Brain Imaging Center, Department of Psychological and Brain Sciences, University of California, Santa Barbara, California*

Submitted 4 January 2012; accepted in final form 26 March 2012

Bernier P-M, Cieslak M, Grafton ST. Effector selection precedes reach planning in the dorsal parietofrontal cortex. *J Neurophysiol* 108: 57–68, 2012. First published March 28, 2012; doi:10.1152/jn.00011.2012.—Experimental evidence and computational modeling suggest that target selection for reaching is associated with the parallel encoding of multiple movement plans in the dorsomedial posterior parietal cortex (dmPPC) and the caudal part of the dorsal premotor cortex (PMdc). We tested the hypothesis that a similar mechanism also accounts for arm selection for unimanual reaching, with simultaneous and separate motor goal representations for the left and right arms existing in the right and left parietofrontal cortex, respectively. We recorded simultaneous electroencephalograms and functional MRI and studied a condition in which subjects had to select the appropriate arm for reaching based on the color of an appearing visuospatial target, contrasting it to a condition in which they had full knowledge of the arm to be used before target onset. We showed that irrespective of whether subjects had to select the arm or not, activity in dmPPC and PMdc was only observed contralateral to the reaching arm after target onset. Furthermore, the latency of activation in these regions was significantly delayed when arm selection had to be achieved during movement planning. Together, these results demonstrate that effector selection is not achieved through the simultaneous specification of motor goals tied to the two arms in bilateral parietofrontal cortex, but suggest that a motor goal is formed in these regions only after an arm is selected for action.

arm reaching movements; parietofrontal network; simultaneous electroencephalogram-functional magnetic resonance imaging

THE ENVIRONMENT AFFORDS US with multiple visual stimuli that can be acted upon. Efficient sensorimotor interactions thus require the brain to be endowed with a potent mechanism for selecting among the many potential actions. Current theoretical models suggest that target selection is associated with the simultaneous specification of multiple potential target goals. In this framework, the selection of a target and the planning of an associated movement would not occur serially in time. Rather, the specification of multiple movement plans would serve as the basis for target selection and constitute an inherent component of the decision process (Cisek 2006). In support of this, spatially selective neuronal populations in reach-related regions of the dorsal parietofrontal cortex show simultaneous encoding of multiple movement plans upon the presentation of multiple visuospatial targets, before reflecting the selected option (Cisek and Kalaska 2002; Klaes et al. 2011; Scherberger and Andersen 2007). Selection would be achieved through mutual inhibition between these populations and the biasing of inputs from other regions.

Address for reprint requests and other correspondence: P.-M. Bernier, Département de Kinanthropologie, Université de Sherbrooke, 2500 boul. de l'Université, Sherbrooke, QC, Canada J1K 2R1 (e-mail: pierre-michel.bernier@usherbrooke.ca).

At the same time, our motor system is inherently redundant: either arm can be used to achieve most of our goals. Yet, the neural mechanisms that contribute to the selection of an effector for action remain largely unknown. One interesting contention is that, similar to the simultaneous representation of multiple target goals, effector selection may be associated with the parallel specification of motor plans for each of the two arms, which would serve as the basis for selection to occur. Support for this possibility comes from electrophysiological studies in monkeys comparing neural activity in conditions in which a visuospatial target can be acquired with either an arm or an eye movement. It has been shown that regions specialized for the planning of each type of movement [i.e., parietal reach region (PRR) for arm movements and lateral intraparietal area for saccades (Andersen and Buneo 2002)] are simultaneously active before an effector is selected, after which only the region corresponding to the selected action maintains elevated levels of activity (Cui and Andersen 2007). Yet, it could be argued that the parallel encoding of arm and eye movements is a natural by-product of the fact that these effectors are typically used in combination in the natural world, with the eyes acquiring a target in conjunction with an arm movement. It thus remains an open question whether more mutually exclusive decisions, such as selecting one of the two arms for a unimanual reaching movement, is also associated with the simultaneous specification of motor plans for the two arms.

In this study we used a two-arm selection reaching task and asked whether effector selection is associated with the simultaneous and separate encoding of motor goals tied to each arm. We used simultaneous electroencephalogram and functional magnetic resonance imaging (EEG-fMRI) and focused on two functionally related regions of the parietofrontal cortex: the dorsomedial part of the posterior parietal cortex [dmPPC; putative parietal reach region (PRR) in monkeys (Bernier and Grafton 2010; Connolly et al. 2003)] and the caudal part of the dorsal premotor cortex (PMdc). In both humans and monkeys, these regions have been shown to contain spatially tuned neurons that are specific to the coding of a motor goal for movements of the contralateral arm (Bernier and Grafton 2010; Beurze et al. 2007; Chang et al. 2008; Connolly et al. 2003; Fabbri et al. 2010; Galletti et al. 1997; Snyder et al. 1997).

The experimental strategy was to compare reaching tasks for which the arm to be used would be selected either before or after a visuospatial target was presented. In the cued condition, subjects were given full knowledge of the arm with a cue provided 2 s before target onset (Fig. 1*A*). Effector selection could thus be achieved before the reaction time (RT) interval (i.e., time between target onset and movement onset). In the uncued condition, subjects had to select the appropriate arm for reaching based on the color of the appearing visuospatial

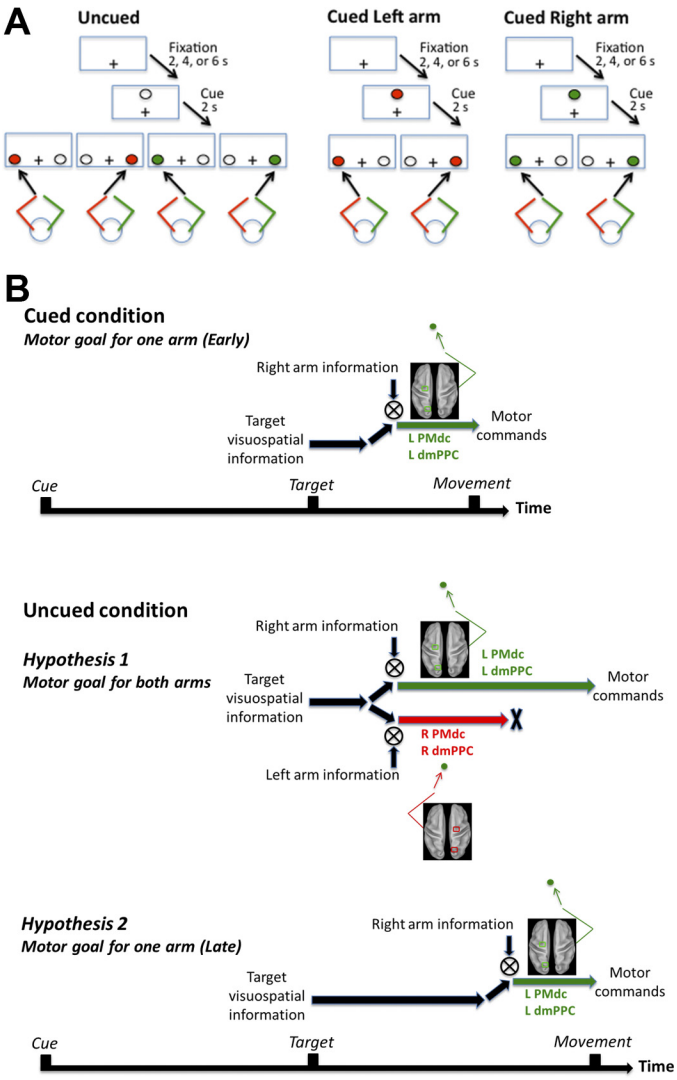

Fig. 1. *A*: task description. Subjects performed reaching movements with their left or right index fingertips toward colored targets presented either left or right of a central fixation point (depicted as "+"). The color of the target instructed which arm to use for the reach (e.g., red target = left arm, green target = right arm). Before each target presentation, a cue was provided for 2 s, the color of which was either noninformative (white; uncued condition) or fully informative (red or green; cued condition) as to the color of the upcoming target, and therefore the arm to be used. *B*: hypotheses. *Top*: cued condition: early specification of a motor goal for a single arm in contralateral dorsomedial posterior parietal cortex (dmPPC) and caudal part of the dorsal premotor cortex (PMdc). When subjects know which arm to use before target onset, the target and arm sensory signals are rapidly integrated in the contralateral dmPPC and PMdc to form a motor goal (Beurze et al. 2007; Chang et al. 2008). We assume that the cued condition incurs negligible specification of a motor goal for the "unselected" arm (i.e., ipsilateral dmPPC and PMdc). *Middle*: uncued condition, *hypothesis 1*: specification of motor goals for both arms in bilateral dmPPC and PMdc. A first possibility is that effector selection is associated with the parallel encoding of motor goals tied to the 2 arms in bilateral dmPPC and PMdc, until 1 is selected for overt execution. This predicts greater activity in dmPPC and PMdc controlling the unselected arm (i.e., ipsilateral dmPPC and PMdc) in the uncued compared with the cued condition. *Bottom*: uncued condition, *hypothesis 2*: late specification of a motor goal for a single arm in contralateral dmPPC and PMdc. A second possibility is that dmPPC and PMdc do not contribute to effector selection but are only recruited to form a motor goal after an arm is selected. This predicts a delay in the recruitment of contralateral dmPPC and PMdc in the uncued compared with the cued condition.

target. Effector selection thus had to be achieved during the RT interval. Our main objective was to test for the transient specification of simultaneous and separate motor goals for each of the two arms in the uncued condition immediately after target presentation. Our analyses thus focused primarily on brain activity occurring during the RT interval.

The first possibility is that the brain simultaneously specifies separate motor goals, one for each arm, before one is selected for overt execution. This predicts that in the uncued condition, the presentation of the visuospatial target would be associated with the transient recruitment of bilateral dmPPC and PMdc, representing both right and left arm movements. The alternative possibility is that a motor goal is only specified for the appropriate arm after it is selected for action. This predicts that in the uncued condition, the presentation of the visuospatial target would be associated with contralateral dmPPC and PMdc recruitment only. Critically, it predicts a difference in the timing of activity in these regions depending on whether arm selection must be achieved after target presentation (uncued condition) or not (cued condition). This timing difference would account for differences in RT across conditions (see Fig. 1*B* for detailed hypotheses).

MATERIALS AND METHODS

Subjects. Eighteen right-handed subjects (11 males, age range 20–32 yr) participated in the simultaneous EEG-fMRI experiment. The EEG data of three subjects were discarded due to excessive noise. The EEG traces are thus the average of data from 15 subjects. All subjects gave informed written consent in accordance with the guidelines from the Human Subjects Committee, Office of Research, University of California, Santa Barbara. The protocols were submitted to an independent review committee for approval. All subjects had normal vision and no history of neurological disease or psychiatric disorders. The subjects were paid for their participation in the study.

Apparatus. Subjects were positioned in the scanner with their head and neck padded with foam to prevent motion. They wore a set of headphones for ear protection and noise cancelation. Visual stimuli were presented on a custom-built board made of thin opaque fiberglass that rested on the subjects' abdomen, so as to be approximately perpendicular to the direction of gaze when looking through the mirrors (distance of the board with respect to the eyes ~35 cm). Subjects were strapped to the table at the level of the chest to prevent excessive movement. The reaches were done in total darkness; hence subjects could not see their reaching hand at any point.

Light-emitting diodes (LEDs), which served as a fixation point, cues, targets, and distractors, were mounted on the stimuli board (Fig. 1*A*). The fixation point was white and was positioned at the center of the board (0° with respect to subjects' body midline). The three cues were white, red, and green and were positioned immediately above the central fixation point. The targets were red or green and could appear at two locations, either 5 cm to the left of the fixation point or 5 cm to its right. Distractors were white and systematically appeared at the location not occupied by a target (see *Task procedures*). The starting position was located perpendicular to the board, 10 cm below the fixation point. It consisted of an MR-compatible button box with two switches that subjects pressed with their left and right index fingertips between each movement. The switches required minimal finger force to be depressed. Subjects were required to gaze at the fixation point throughout the trials; hence reaches were always performed toward targets viewed in the peripheral visual field. The visual angle subtended by the targets from the fixation point was ~8°. The amplitude of the reaches was short (~10 cm) so that they could be accomplished mostly through wrist rotation, thereby minimizing motion of the upper arm. Yet subjects physically displaced their hand to touch the targets,

justifying our use of the term "reaching" instead of "pointing" [i.e., angling the finger in the direction of the target without touching it (Culham et al. 2006)].

Task procedures. Subjects performed reaching movements with their left or right index fingertips toward colored targets. A choice RT task was used in which a colored target and a white distractor always appeared on every trial. Subjects had to reach to the target, and never to the distractor. The presence of distractors was designed to balance the visuospatial activity presented in the left and right hemifields on each trial. Thus potential hemispheric asymmetries in PPC activity could not be attributable to differences in sensory stimulation. The color of the target instructed which arm to use for the reach. For instance, a red target designated a right arm reach, whereas a green target designated a left arm reach. This arbitrary color-arm mapping was fixed for the entire experiment for each subject but was counterbalanced across subjects. Subjects' knowledge regarding the arm to be used for an upcoming reach was manipulated by presenting a cue before target onset. In half of the trials (cued condition), the cue was the same color as that of the upcoming target (red or green). Thus the cue was fully informative as to which arm would be used for the reach. In the other half of the trials (uncued condition), the cue was white and noninformative as to the arm to be used. In sum, all trials fell evenly into a two-cue (cued, uncued) × two-arm (left, right) × two-target (left, right) factorial design.

In light of current models suggesting that selection is not separate from the planning of the movement (Cisek and Kalaska 2002; Klaes et al. 2011; Scherberger and Andersen 2007), we chose to use a rapid event-related design. This emphasized natural sensorimotor processes without requiring "artificial" delays between selection and planning, as is the case for slow event-related fMRI designs.

Before each trial, subjects were required to bring their left and right index fingertips to the starting position and press the button box switches. If subjects failed to press the switches, a trial would not start, allowing us to maintain some control over the flow of the experiment (<2% of trials for all subjects). While subjects gazed at the fixation point, the cue (red, green, or white) was provided for 2 s. After this delay, a target and a distractor appeared and subjects initiated their reach as quickly and accurately as possible while keeping their gaze on the fixation point. The target and distractor disappeared on movement initiation (as recorded by the release of the switches). Subjects were told to produce straight and smooth movements, to physically touch the board briefly at the end of their movement, and to then bring their fingers back to the starting position for the next trial. The out-and-back movement was generally achieved in <2 s. The intertrial interval was jittered between three possible durations of 2, 4, or 6 s.

The study comprised two experimental sessions, carried out on separate days. In the first practice session, the blood oxygen level-dependent (BOLD) fMRI signal was recorded while subjects produced the reaching movements in a block design. EEG signals were not recorded during this session. The practice session consisted of four blocks of reaching and two blocks of passive viewing (no reaching). Each block lasted 300 s and was made up of 6 segments of 30 s in which the targets and distractors were presented 8 times, interleaved with 20-s breaks in which no targets were presented. In the four reaching blocks, subjects reached toward the targets after their appearance. Each of the two-arm × two-target conditions was done in separate blocks. In the passive viewing blocks, subjects remained passive while the targets were presented. Subjects were instructed not to covertly plan a reach toward the targets, but to simply keep gazing at the fixation point while targets were presented. Together, these blocks allowed us to isolate the brain areas specifically recruited for the planning of arm reaching movements vs. those merely associated with passive viewing of visual stimuli in peripheral vision. They also allowed subjects to familiarize with the task (i.e., gazing at the fixation point during the reaches, producing smooth movements).

In the main experimental session, the BOLD and EEG signals were simultaneously recorded while subjects produced the reaching movements in each of the two-cue × two-arm × PPC (two 2-target conditions). Reaches were performed in five separate runs. Four runs consisted of 100 trials and one run consisted of 96 trials, for a total of 496 trials. This corresponded to 62 reaches in each of the cue × arm × target conditions. A 30-s break was provided in the middle of each run to allow subjects to rest. The total time of each run was ~720 s. The sequence of presentation of the trials as well as the intertrial interval was pseudorandomized using an m-sequence (Buracas and Boynton 2002; Liu 2004), ensuring that the design matrices of both the general linear model (GLM) and deconvolution analyses were invertible and had a unique solution for each time point. The orthogonality of the design matrices was assessed before data collection to ensure adequate power to detect BOLD activations for all conditions of interest.

Behavioral analyses. RT was defined as the time between target onset and movement onset, as measured by the release of the button box switches. Trials in which subjects reached with the wrong arm were discarded from further analyses (assessed by the button box switches; <3% of trials for all subjects). Importantly, errors were not more common in the uncued than in the cued condition ($P > 0.2$), which rules out a potential congruence effect between the color of the cue and that of the target. RT data were submitted to a two-cue × two-arm × two-target repeated-measures analysis of variance (ANOVA). The threshold for statistical significance was set to 0.01.

MRI scanning and analyses. Functional MRI recordings were conducted using a Siemens 3T Magnetom TIM Trio system with a 12-channel phased-array head coil. For each functional run, a T2-weighted echo planar gradient-echo imaging sequence sensitive to BOLD contrast was acquired [repetition time (TR) = 2,000 ms, echo time (TE) = 30 ms, flip angle (FA) = 90°, field of view (FOV) = 192 mm]. Each volume consisted of 37 slices acquired parallel to the anterior and posterior commissure (AC-PC) plane (interleaved acquisition; 3 mm with 0.5-mm gap; 3 × 3-mm in-plane resolution). Before the functional runs, a high-resolution T1-weighted sagittal sequence image of the whole brain was acquired (TR = 15 ms, TE = 4.2 ms, FA = 9°, FOV = 256 mm).

Functional MRI data preprocessing and statistical analyses were carried out in SPM5 (www.fil.ion.ucl.ac.uk/spm). The first three functional volumes of each run were automatically removed by the operating system software to eliminate nonequilibrium effects of magnetization, before the start of the task. Individual scans were spatially realigned to the middle image of the time series, slice-time corrected, registered to the anatomic image, and normalized to Montreal Neurological Institute (MNI) space (resampled at 3 × 3 × 3-mm resolution). Images were temporally high-pass filtered with a 128-s cutoff. The functional data were then smoothed with an 8-mm full-width half-maximum isotropic Gaussian kernel. Finally, even with the head perfectly stable, the dislocation of a mass near but outside the head coil can induce signal changes in the images. We thus utilized a weighted least-squares algorithm to weigh each image by the inverse of its variance, therefore minimizing the impact of outlier images in the estimation of the GLM (Diedrichsen and Shadmehr 2005).

First-level whole brain fMRI analyses, estimated for each subject individually, sought to identify brain regions associated with reach planning. With the use of a GLM, the fMRI time series was fitted with eight regressors (and their temporal derivatives) corresponding to each of the cue × arm × target conditions. The events were defined as the onset of the target and were modeled with RT as duration. Separate regressors of noninterest were also added to account for error trials, the effect of multiple scanning runs, and MR drift. Each event was convolved with the standard gamma-shaped hemodynamic response function (HRF) and its temporal derivative.

Because the hypotheses regarding dmPPC function predicted a change in either the amplitude or the latency of the response as a function of cue condition (see Fig. 1*B*), we analyzed both these

components of the BOLD response separately. The amplitude of the BOLD response was calculated by incorporating both the nonderivative and derivative terms of the model. This has been shown to minimize the latency-induced amplitude bias associated with spatially varying hemodynamic delays (Calhoun et al. 2004). The latency of the BOLD response was assessed by comparing the magnitude of the derivative term of the model across cue conditions. A positive loading of the derivative term indexes a BOLD response that is shifted earlier in time, and vice versa. This analysis was restricted to the regions that responded significantly to the task and was thus carried out using an inclusive mask of the regions that showed a significant nonderivative term.

For each subject, brain activity in each of the four arm-target conditions was first assessed by contrasting these conditions to baseline (left arm, left target; left arm, right target; right arm, left target; right arm, right target). In separate independent analyses, we then assessed the effect of the cue (cued vs. uncued) on reach planning activity. Given the large differences in brain activity as a function of arm but not as a function of target (see RESULTS), these analyses were carried out separately for left and right arm reaching, but by pooling across left and right targets. The main contrasts were thus left arm uncued vs. left arm cued and right arm uncued vs. right arm cued. For each subject, these contrasts were done on both the amplitude and the latency components of the BOLD response.

A second-level random-effects analysis was then applied to individual contrasts of parameter estimates (separately for the amplitude and latency components) to obtain a population estimate. All reported statistics are corrected for false discovery rate at $q(\text{FDR}) < 0.05$ (Genovese et al. 2002), unless a more stringent threshold is stated.

Because the interaction between response amplitude and latency is complex (Calhoun et al. 2004; Lindquist et al. 2009), we sought to confirm the latency differences obtained in the main GLM analysis using an independent model. To do this, we used a deconvolution analysis that makes no assumptions with respect to the HRF, allowing us to gain insight into the true shape of the BOLD response. The deconvolution analysis was done using AFNI's 3dDeconvolve (http://afni.nimh.nih.gov/afni/). This analysis was performed on four key regions within the dorsal parietofrontal network that were isolated with the amplitude and latency contrasts from the GLM, namely, the rostral part of the dorsal premotor cortex (PMdr), the PMdc, the medial part of the medial intraparietal sulcus (mIPS), and the dmPPC. These functional regions of interest were defined based on clusters of significant voxels from the second-level random-effects analysis. Because these regions were highly symmetric across the two arms (i.e., same cortical area for left and right arm reaching but in different hemispheres), they were collapsed for further quantitative analyses. Impulse functions time locked to the onset of the targets were used as event onsets, and the BOLD response was estimated for 12 s poststimulus, using 6 tent functions of 1-TR duration spaced 2 s apart (essentially delta functions, allowing for optimal temporal precision). Paired-samples *t*-tests were used to statistically assess the time points at which a significant amplitude difference occurred across conditions ($P < 0.05$; Bonferroni corrected). To assess changes in the latency of the BOLD response, we calculated the normalized area under the curve (AUC) for each subject. Paired-samples *t*-tests were then used to determine the time points at which a significant difference existed across conditions ($P < 0.05$; Bonferroni corrected).

For visualization purposes, the *t*-images were mapped to the partially inflated cortical surface of the Population-Average Landmark- and Surface-based (PALS-B12) atlas (Van Essen 2005) using the Caret software application. The PALS-B12 atlas represents the surface registration of 12 normal adult high-resolution scans, which can be used as an unbiased template for displaying images from group fMRI analyses. Because the a priori-defined hypotheses were restricted to cortical areas, only regions within the cortex are reported (although the fMRI statistics derive from whole brain analyses).

EEG data acquisition and analyses. EEG was acquired simultaneously with fMRI using a 64-channel MR-compatible BrainAmp system (Brainproducts, Munich, Germany) along with the BrainCap electrode cap (Falk Minow Services, Herrsching-Breitbrunn, Germany). When placing the cap, we made sure that the Cz electrode was at the vertex. The electrodes were ring-type sintered nonmagnetic Ag-AgCl electrodes and were positioned in accordance with the extended 10/20 system. The reference electrode was located between Fz and Cz. Vertical eye movements and blinks were monitored with frontal electrode FP2 (positioned above the right orbit), whereas horizontal eye movements were monitored with electrodes positioned near the left and right outer canthi, respectively. An electrocardiogram (ECG) electrode was placed on the subjects' back at the level of the heart. The EEG and ECG signals were digitized online (sampling rate 5 kHz), and impedances were kept below 20 kΩ.

EEG data were analyzed off-line using the Brain Vision Analyzer software (version 2.0; Brainproducts). The data were first corrected for MR gradient artifacts using an adaptive artifact subtraction method (Allen et al. 2000). Data were also down-sampled to 256 Hz. The EEG data were then corrected for cardioballistic artifacts using an average subtraction method (Allen et al. 1998). Trials in which horizontal eye movements occurred during the RT interval were removed (<1% of trials for all subjects). Subjects were encouraged to delay their blinks until the intertrial interval, yet remaining ocular artifacts were subtracted from the EEG signal using the statistical method of Gratton et al. (1983). The data were visually inspected for remaining artifacts resulting from other muscular sources. They were digitally bandpass filtered off-line (0.1–35 Hz, notch at 50 Hz, 12 dB/octave) and transformed to the average reference. The ECG channel as well as FP1, FP2, TP9, and TP10 were not included for further analyses.

The data were averaged within a window between −0.4 and +0.8 s around the onset of the target to obtain event-related potentials (ERPs). To visualize scalp distributions over time, topographical current source density (CSD) maps were computed using Laplacian transformation (Babiloni et al. 2001) with Brain Vision Analyzer. The signal was interpolated with a spherical spline interpolation procedure (Perrin et al. 1987) to compute second-order derivatives in two dimensions of space (order of splines: 3; maximal degree of Legendre polynomials: 10; approximation parameter λ: 1.0e−005). CSDs are independent of the reference electrode site and are much less affected by far-field generators than monopolar recordings (Manahilov et al. 1992). They are therefore considered to provide a better reflection of the underlying cortical activities.

The main focus of the EEG analysis was to provide further insight into the temporal dynamics of activity in the parietal and premotor regions identified in the fMRI analyses. To identify the parietal activations, we pooled the electrodes overlaying the left (P1, P3, PO3) and right PPC (P2, P4, PO4). To identify the precentral activations, we pooled the electrodes overlaying the left (FC1, FC3, C1) and right PMdc (FC2, FC4, C2) [see Homan et al. (1987) for the cerebral topography of the electrodes]. These data were then collapsed across left and right arm reaching and referred to as ipsilateral or contralateral to the reaching arm.

To further scrutinize the underlying sources giving rise to the EEG signal, we used ERP dipole source analysis with BESA (Brain Electrical Source Analysis version 2; http://www.besa.de), using a four-shell elliptical head model (Berg and Scherg 1994). The sources seeded into BESA corresponded to the centroids of the regions that showed a significant latency difference in BOLD response across cue conditions in the GLM analysis, namely, dmPPC and PMdc (see RESULTS). To confirm that these latency differences were specific to these regions, dipoles were also seeded in mIPS to act as controls, because mIPS showed an amplitude difference but not a latency difference in BOLD response across cue conditions. The peak MNI coordinates of these regions were converted into Talairach coordinates using the Talairach deamon (http://www.talairach.org/) (Lancaster et al. 1997, 2000). By keeping the location of the dipoles

constant and by varying only their orientation, the source analysis allowed us to find the set of orientations that accounts for the most variance in the EEG data. The fits were calculated for all dipoles simultaneously in a time window between target onset and response onset. The source analysis was applied to the grand average as well as the single-subject traces for the cued and uncued conditions, separately for both arms. The traces were then collapsed across left and right arms and relabeled as ipsilateral or contralateral to the reaching arm.

To assess the relationship between brain activity and movement onset, a correlation analysis was performed between each subject's RT and their timing of peak activity in dmPPC and PMdc (taken from source analysis waveforms). Specifically, we correlated the difference in peak timing in these regions between the cued and uncued conditions with the difference in RT in the cued and uncued conditions. This analysis was carried out separately for dmPPC and PMdc. This difference measure allowed us to control for interindividual variability in baseline performance. The peak timing was identified for each subject within a window centered around the peak of the grand-average dmPPC and PMdc waveforms plus or minus one standard deviation. Because we did not have an estimate of the variance around the peak of these activities (there was a single grand average), the variance in subjects' RT was used. A nonparametric Spearman's rank correlation coefficient test was used to assess the statistical significance of the relationship. Of the 15 subjects for whom we had simultaneous EEG data, 3 did not present single discernible peaks in either dmPPC or PMdc activity within the variance interval. These subjects were not included in the correlation analysis, which was thus carried out on 12 subjects for dmPPC and PMdc.

RESULTS

Reaction time. The three-way ANOVA revealed only a main effect of cue. Subjects were slower to initiate their responses in the uncued (mean RT: 619 ± 85 ms) than in the cued condition (mean RT: 470 ± 95 ms) [$F_{(1,17)} = 145.2$, $P < 0.0001$], consistent with the additional computation required to select the appropriate arm in the uncued condition. There were no significant main effects of arm or target.

Functional MRI. With the use of data from the main experimental session, the brain areas recruited for each combination of arm and target were initially assessed. The arm used for reaching incurred significant activity in the contralateral sensorimotor cortex as well as in many regions of the parietal and frontal cortex. These included the superior parietal lobule (SPL), the inferior parietal lobule (IPL), the dorsal and ventral

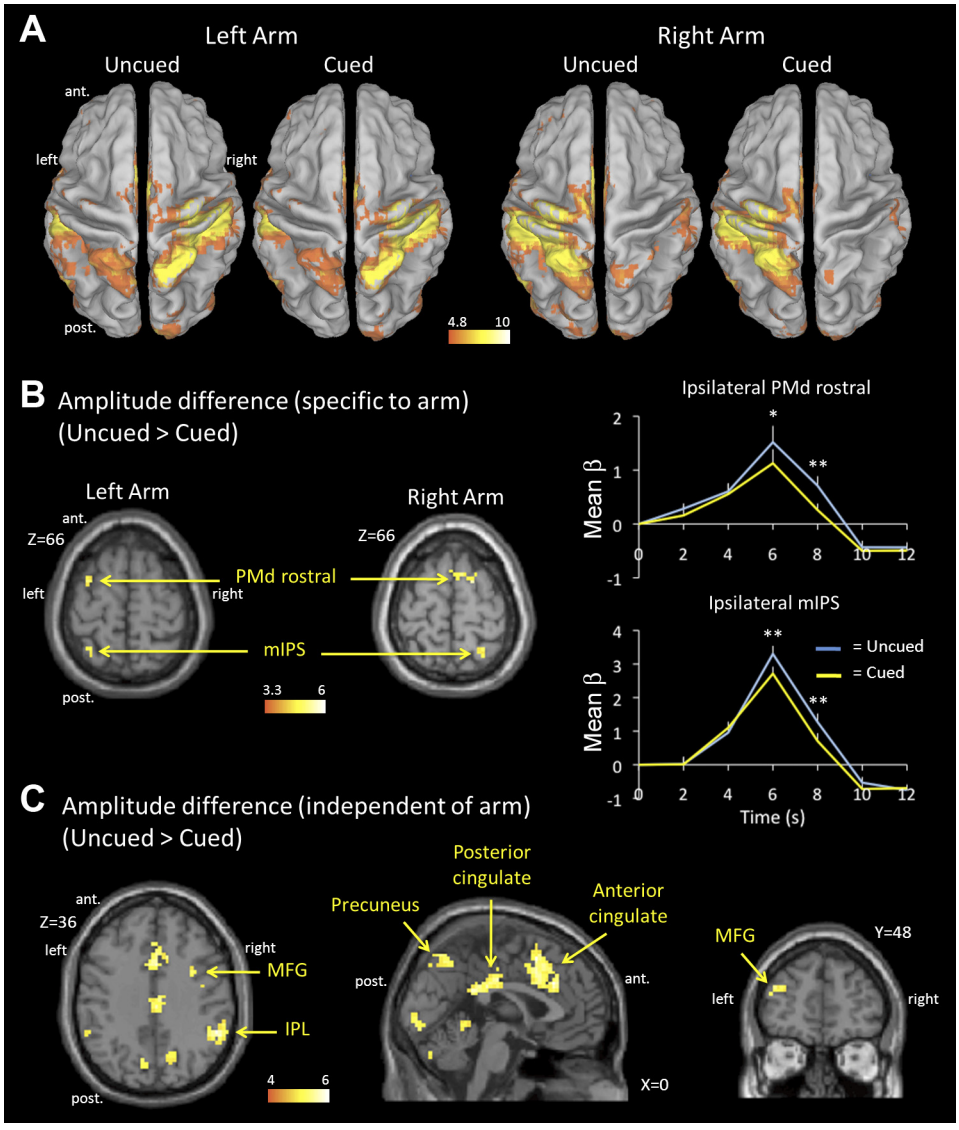

Fig. 2. Amplitude of the blood oxygen level-dependent (BOLD) response. *A*: areas showing significant BOLD response in each of the cue × arm conditions compared with baseline ($P < 0.05$ family-wise error corrected). *B*, *left*: areas showing significantly greater BOLD response in the uncued than in the cued condition, shown for the left and right arms separately [$P < 0.05$ false discovery rate (FDR) corrected]. *Right*: deconvolved BOLD response for PMd rostral and mIPS ipsilateral to the reaching arm in the uncued and cued conditions (data collapsed across the 2 arms). *C*: areas showing significantly greater BOLD response in the uncued than in the cued condition, irrespective of the reaching arm ($P < 0.05$ FDR corrected; no significant activation for the contrast cued > uncued). *$P < 0.05$; **$P < 0.005$. IPL, inferior parietal lobule; MFG, middle frontal gyrus; mIPS, medial intraparietal sulcus; ant., anterior; post., posterior.

Table 1. *Average MNI coordinates of clusters showing significantly more activity in the uncued compared with the cued condition*

Anatomic Region	Functional Label (Brodmann area)	Hemisphere	MNI Coordinates			*t* Value
			x	*y*	*z*	
		Left arm reaching				
Middle frontal gyrus	BA 10/BA 9	Left	−39	48	24	3.62
Middle frontal gyrus	BA 10/BA 9	Right	42	51	24	3.85
Middle frontal gyrus	PMd rostral (BA 6)	Left	−30	6	66	3.51
Cingulate gyrus	Anterior cingulate (BA 32)	Right	3	24	39	4.14
Cingulate gyrus	Posterior cingulate (BA 23)	Right	6	−21	30	4.59
Intraparietal sulcus	mIPS (BA 7)	Left	−30	−54	60	3.46
Inferior parietal lobule	BA40	Left	−51	−51	42	3.78
Inferior parietal lobule	BA40	Right	54	−45	36	4.18
Superior parietal lobule	Precuneus (BA 7)	Right	6	−63	48	3.45
Lingual gyrus	BA 17	Right	3	−90	−3	3.78
		Right arm reaching				
Middle frontal gyrus	BA 46	Left	−45	39	24	3.52
Superior frontal gyrus	BA 9	Right	27	54	30	3.68
Superior frontal gyrus	PMd rostral (BA 6)	Right	18	3	66	4.42
Cingulate gyrus	Anterior cingulate (BA 32)	Left	−3	15	39	5.07
Cingulate gyrus	Posterior cingulate (BA 23)	Right	3	−24	36	4.95
Intraparietal sulcus	mIPS (BA 7)	Right	27	−54	66	3.73
Inferior parietal lobule	BA40	Left	−36	−57	45	4.2
Inferior parietal lobule	BA40	Right	60	−36	33	4.38
Superior parietal lobule	Precuneus (BA 7)	Left	−6	−72	48	4.62

Montreal Neurological Institute (MNI) coordinates are in mm. All activations are significant at $P < 0.05$ false discovery rate (FDR) corrected; minimum cluster size, 10 voxels. PMd, dorsal premotor cortex; mIPS, medial intraparietal sulcus.

aspects of the premotor cortex (PMd and PMv, respectively), the supplementary motor area (SMA), the anterior and posterior cingulate, and the middle frontal gyrus (MFG). These regions were primarily observed in the hemisphere contralateral to the reaching arm, although the activation was more bilateral for left arm reaching than right arm reaching. Overall, this pattern of activity supports the prominent role played by the left hemisphere for action (Krams et al. 1998; Rushworth et al. 2001). In contrast, the influence of the spatial position of the target was negligible. As observed in previous work from our group (Bernier and Grafton 2010), reaching to a target across the body midline was only associated with greater activity in bilateral postcentral gyrus [Brodmann area 5 (BA 5)] compared with reaching to a target ipsilateral to the arm. It is likely that the relatively small target location effect was attributable to the fact that visuospatial signals were balanced in each hemisphere, since a target was always accompanied by a distractor.

The main objective of the present study was to test the hypothesis that effector selection is associated with the parallel specification of motor goals tied to the two arms in bilateral dmPPC, which we assessed by comparing neural activity during the RT interval between the cued and uncued conditions. Given the large differences in BOLD response as a function of arm but not as a function of target location, these analyses were carried out separately for the two arms, but by pooling across the two target dimensions (see MATERIALS AND METHODS).

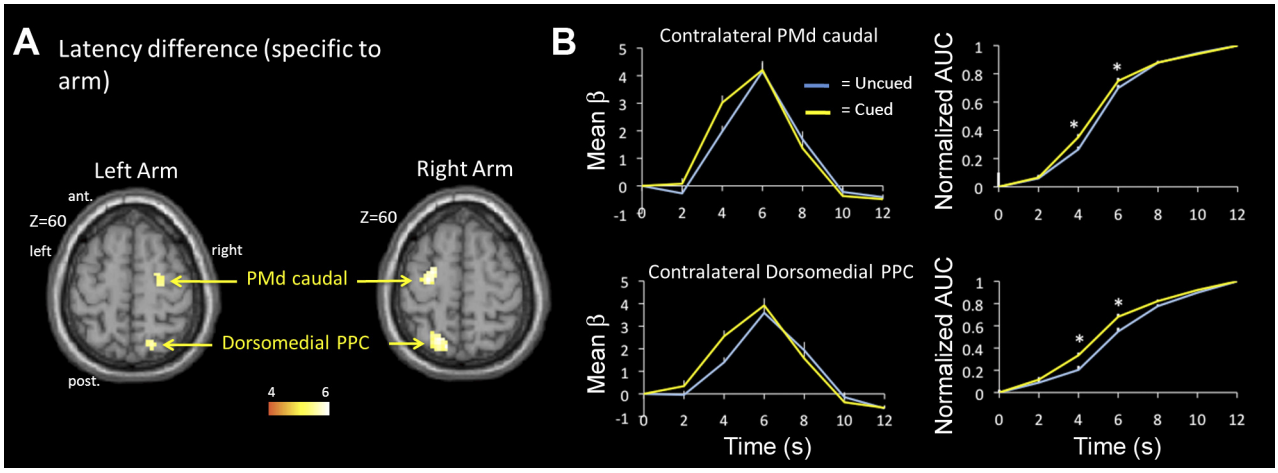

Fig. 3. Latency of the BOLD response. *A*: areas showing significantly delayed BOLD response in the uncued with the cued condition, shown for the left and right arms separately ($P < 0.05$ FDR corrected). *B*, *left*: deconvolved BOLD response for PMd caudal and dmPPC contralateral to the reaching arm in the uncued and cued conditions (data collapsed across the 2 arms). *Right*: normalized area under the curve (AUC) of the BOLD response for PMd caudal and dmPPC contralateral to the reaching arm in the uncued and cued conditions. *$P < 0.005$.

Table 2. *Average MNI coordinates of clusters showing significantly delayed BOLD response in the uncued compared with the cued condition*

Anatomic Region	Functional Label (Brodmann area)	Hemisphere	MNI Coordinates			*t* Value
			x	*y*	*z*	
		Left arm reaching				
Precentral gyrus	PMd caudal (BA 6)	Right	24	−15	63	5.04
Superior parietal lobule	dmPPC (BA 7)	Right	18	−66	60	4.69
		Right arm reaching				
Precentral gyrus	PMd caudal (BA 6)	Left	−27	−12	60	6.04
Superior parietal lobule	dmPPC (BA 7)	Left	−18	−69	54	6.13

All activations are significant at $p < 0.05$ FDR corrected; minimum cluster size, 10 voxels.

First, using data from the main experiment, we assessed differences in the amplitude of the BOLD response as a function of cue condition. Figure 2*A* presents the areas showing a significant BOLD response (with respect to baseline) in each of the cue × arm conditions. Within the dorsal parietofrontal network, two regions were more active in the uncued compared with the cued condition (Fig. 2*B*). One was located in the rostral part of the PMdr (BA 6), with maxima on the medial and lateral banks of the superior frontal sulcus. The other was located in the middle part of the mIPS (BA 7). Importantly, these regions were observed only in the hemisphere ipsilateral to the reaching arm (i.e., contralateral to the "unselected" arm). For left arm reaching, the MNI coordinates of peak maxima were [−30, 6, 66] for left PMdr and [−30, −54, 60] for left mIPS. For right arm reaching, the MNI coordinates were [18, 3, 66] for right PMdr and [27, −54, 66] for right mIPS.

In addition to these two regions in the dorsal parietofrontal network, several other regions were more active in the uncued than cued condition (Fig. 2*C* and Table 1). These comprised the bilateral MFG (BA 9, 10, and 46), posterior cingulate (BA 23), anterior cingulate (BA 32), bilateral IPL (BA 40), and precuneus (BA 7). These regions may have participated in the cognitive process associated with the selection of the correct arm based on the color of the target. No region showed greater BOLD response in the cued than in the uncued condition.

Interestingly, using data from the practice session, in which the BOLD response was recorded during the passive viewing of visual targets being presented with no requirement to plan a movement, we found that mIPS was also recruited. As shown in Fig. 4*B*, the left and right mIPS (peaks at [−30, −51, 60] and [30, −51, 60], respectively) were isolated by doing a conjunction between the regions that were active for both left and right arm reaching, masked inclusively by those active in the passive viewing condition. The fact that this region was recruited during both active reaching and passive viewing suggests that its role in visuomotor transformations may be more tightly linked to the representation of visuospatial target locations, rather than the specification of a motor goal per se.

Second, using data from the main experiment, we assessed differences in the latency of the BOLD response as a function of cue condition. Only two regions showed a significantly delayed BOLD response in the uncued compared with the cued condition (Fig. 3 and Table 2). They were observed contralateral to the reaching arm for both arms. One was located in the dmPPC (BA 7), at coordinates closely corresponding to those identified as the putative homolog of the monkey PRR (left arm: [18, −66, 60]; right arm: [−18, −69, 54]) (Connolly et al. 2003). The other was located in the PMdc (BA 6), at the junction of the precentral sulcus and superior frontal sulcus (left arm: [24, −25, 63]; right arm: [−27, −12, 60]). This latency difference can be seen in Fig. 3*B*, where the BOLD response is shifted rightward (i.e., delayed) in the uncued compared with the cued condition. The AUC analysis statistically confirmed this change in latency, because the ratio of the

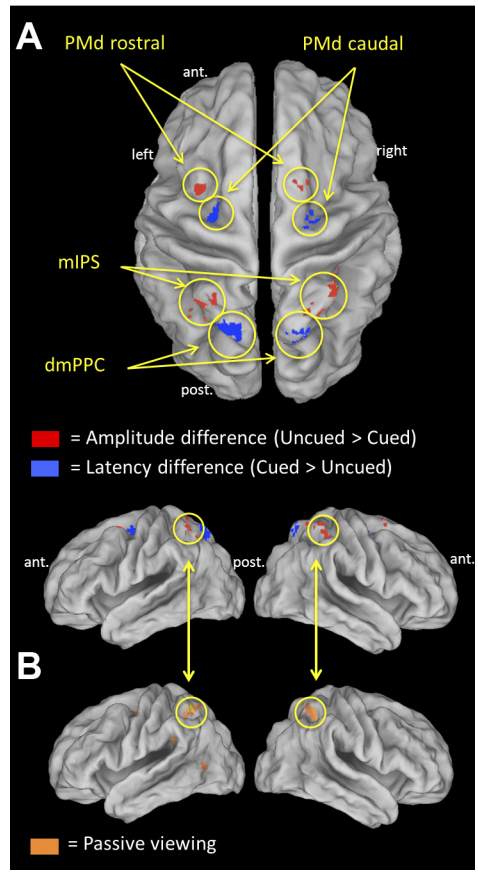

Fig. 4. Regions of interest. *A*: topography of areas showing a significant amplitude difference (mIPS and PMd rostral; shown in red) and latency difference (dmPPC and PMd caudal; in blue) across cue conditions, overlaid on an inflated cortical surface ($P < 0.05$ FDR corrected). *B*: regions activated during left and right arm reaching as well as during passive viewing of visual stimuli. A region corresponding to the mIPS (circled) was isolated in this active/passive conjunction ($P < 0.05$ FDR corrected).

AUC at 4 and 6 s poststimulus was significantly less in the uncued than in the cued condition, in both PMdc and dmPPC ($P < 0.005$).

Overall, the parietofrontal regions showing amplitude (PMdr, mIPS) and latency differences (PMdc, dmPPC) across cue conditions were adjacent to each other and did not overlap. In Fig. 4*A*, their relative topography can be appreciated on an inflated brain.

EEG. EEG was used to add temporal precision in characterizing the time-course of activity in the contralateral dmPPC and PMdc, which showed a delayed BOLD response in the uncued compared with the cued condition. In Fig. 5*A*, the CSD maps associated with right arm reaching in the cued and uncued conditions are presented. It can be seen that a left parietooccipital positive potential and a left frontal negativity develop at ~375 ms in the cued condition but at ~475–525 ms in the uncued condition. The CSD traces averaged over the electrodes overlaying the contralateral parietal and precentral regions are presented in Fig. 5*B*. It can be clearly observed that the positivity over the parietal electrodes contralateral to the reaching arm peaked later in the uncued (508 ms) than in the cued condition (380 ms). The negativity over contralateral precentral electrodes also peaked later in the uncued (448 ms) than in the cued condition (388 ms). No difference was observed in the parietal or precentral region ipsilateral to the reaching arm. It could be argued that these latency differences result from poor averaging due to greater interindividual variability in RT in the uncued condition. However, the data do not support this contention, because RT was actually less variable across subjects in the uncued (SD = 85 ms) than in the cued condition (SD = 95 ms). No such timing difference between cued and uncued conditions was observed in either the parietal or precentral region ipsilateral to the reaching arm.

To quantify these temporal differences, we used a source analysis modeled on the regions of interest isolated in the fMRI analysis. Source analysis was performed on three pairs of dipoles with seeds corresponding to the centroids of the bilateral dmPPC, PMdc, and mIPS activations (see dipole locations in Fig. 6, *inset*). Iterative best-fit modeling of the orientation of these dipoles was then applied to the ERP distributions while keeping their location fixed. The explained variance was similar across conditions, ranging from 75 to 79%. In support of the fMRI (see Fig. 3) and CSD results (see Fig. 5), this analysis revealed a clear latency difference in contralateral dmPPC and PMdc as a function of cue condition (see horizontal red arrows in Fig. 6). Specifically, the timing of peak activity in dmPPC occurred significantly later in the uncued (492 ms) than in the cued condition (364 ms) ($P < 0.005$). A similar finding was also observed for PMdc (484 and 384 ms for uncued and cued conditions, respectively; $P < 0.005$). A key control here is that, as in the fMRI data, no latency change was observed in the contralateral mIPS despite its proximity to the contralateral dmPPC, supporting the specificity of the latency effects observed in the dmPPC and PMdc. The pattern of activity in the ipsilateral mIPS was also in good agreement with the fMRI results (see Fig. 2*B*), because there was a tendency for a greater response in the uncued compared with the cued condition ($P > 0.15$; see vertical arrow in Fig. 6). Consistent with the fMRI findings, no difference was observed in the ipsilateral PMdc and ipsilateral dmPPC ($P > 0.2$ for both).

Overall, the difference in the timing of peak activity in contralateral dmPPC and PMdc between cued and uncued conditions (128 and 104 ms, respectively) was roughly consistent with the difference in RT across conditions (149 ms). One possibility is that these regions were only recruited to form a motor goal once an effector was selected for action. If this is

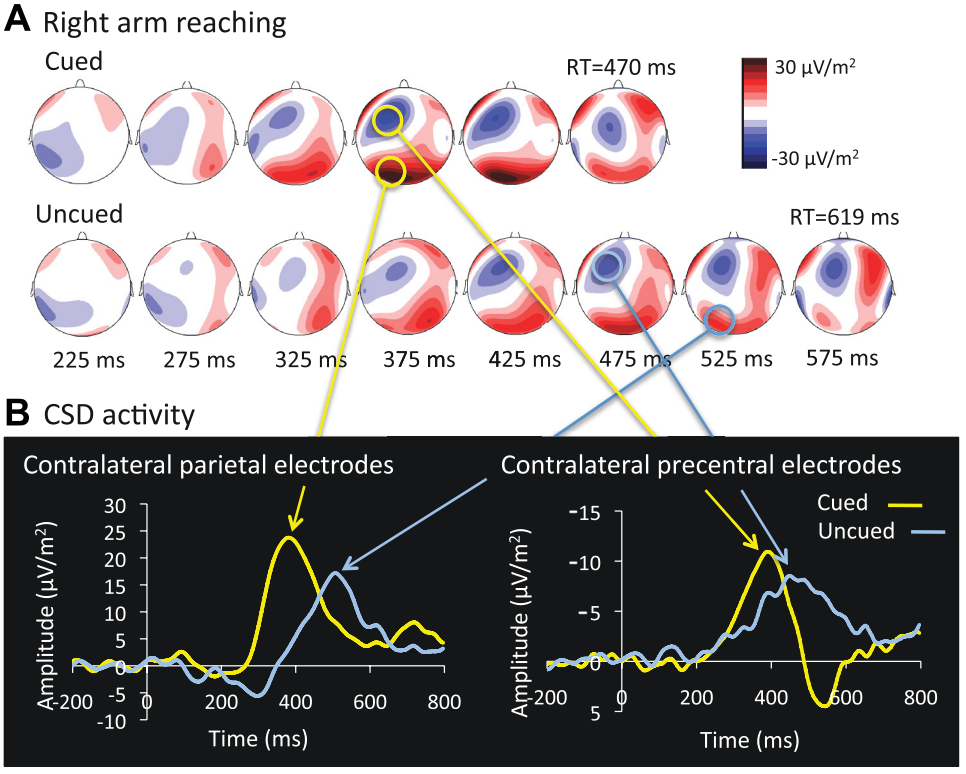

Fig. 5. Current source density (CSD) activity. *A*: scalp topographies of CSD activity time-locked to target onset in the cued and uncued conditions for right arm reaching. In the cued condition, a negativity over left precentral regions and a positivity over left parietal regions are evident at ~375 ms. In the uncued condition, CSD activity at these scalp sites is delayed, with peaks at ~475–525 ms. *B*: CSD traces of contralateral parietal and precentral electrodes in the cued and uncued conditions. Note that data for the 2 arms are collapsed into a single estimate (see MATERIALS AND METHODS). RT, reaction time.

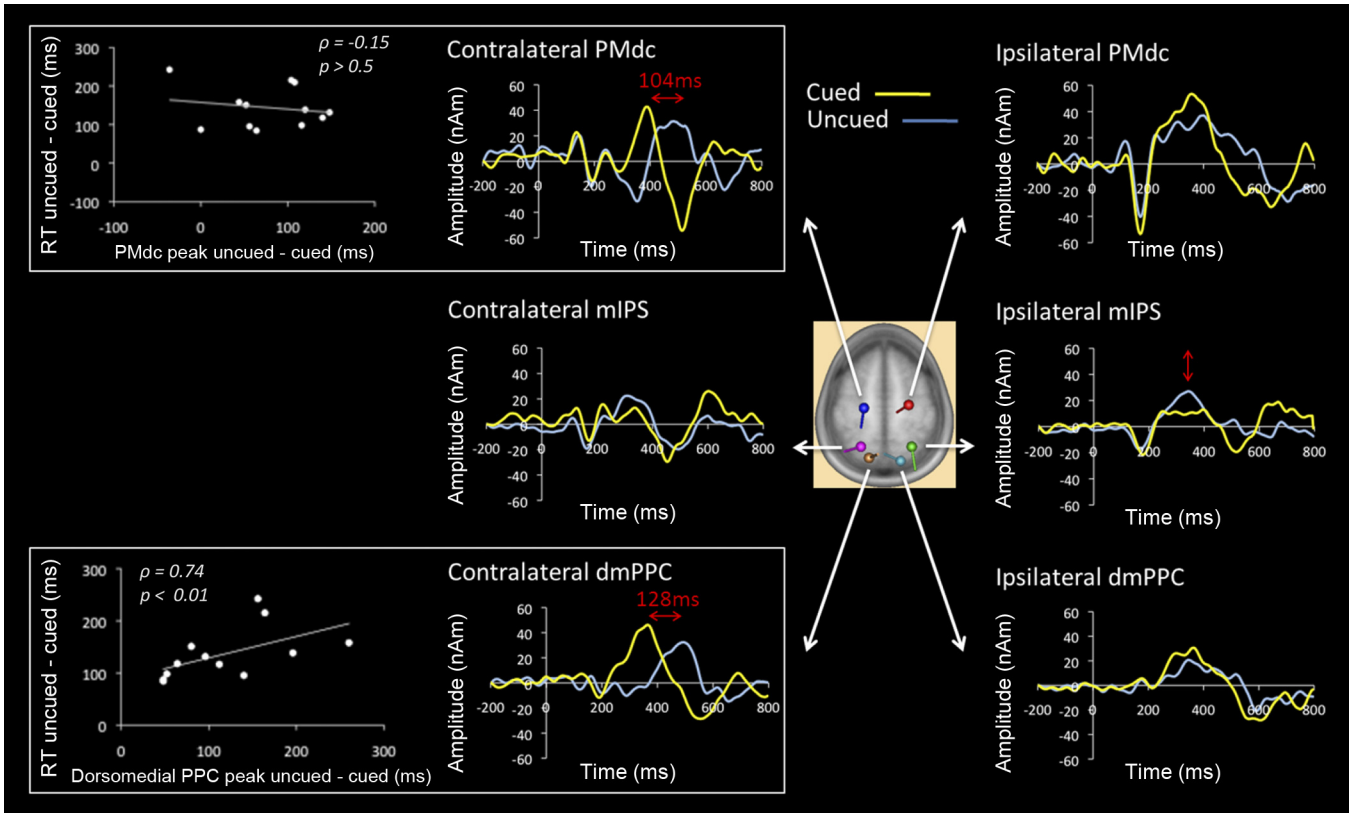

Fig. 6. Functional magnetic resonance imaging (fMRI)-informed source analysis. Source waveforms are shown in the cued and uncued conditions for bilateral PMdc, mIPS and dmPPC. *Center*: location of the dipoles, taken from the coordinates of peak activity in these regions in the fMRI analysis, superimposed on an average brain. Note that data for the 2 arms are collapsed into a single estimate (see MATERIALS AND METHODS). In support of the fMRI and CSD results, the source analysis confirmed the difference in the timing of peak activity in the contralateral PMdc and dmPPC as a function of cue condition (horizontal red arrows in boxed graphs). Graphs at *left* present the correlation between each subject's difference in the timing of peak activity between cue conditions and the difference in RT between cue conditions, shown for the contralateral PMdc (*top*) and dmPPC (*bottom*). The difference in the timing of dmPPC recruitment between cued and uncued conditions predicted well the difference in RT across these conditions ($P < 0.01$). This was not the case for PMdc ($P > 0.5$).

so, then the delay in the timing of activity in these regions should predict the delay in movement onset. To test this, we correlated each subjects' difference in the peak timing of activity between the cued and uncued conditions with their difference in RT between the cued and uncued conditions (Fig. 6, *left*). As can be seen, the delay in dmPPC recruitment reliably predicted the delay in movement onset ($\rho = 0.74$, $t = 3.48$, $P < 0.01$). However, this was not the case for PMdc ($\rho = -0.15$, $P > 0.5$).

DISCUSSION

The dmPPC and PMdc integrate target and arm sensory signals to generate a motor goal for reaching movements of the contralateral arm (Bernier and Grafton 2010; Beurze et al. 2007; Chang et al. 2008; Connolly et al. 2003; Fabbri et al. 2010; Galletti et al. 1997; Snyder et al. 1997). Recent evidence suggests that these regions play a key role in target selection by specifying a range of potential goals that can be acted upon (Klaes et al. 2011; Scherberger and Andersen 2007). We tested the hypothesis that they also contribute to effector selection by simultaneously representing movement plans in both hemispheres, each tied to the contralateral arm. We used an arm reaching task requiring subjects to select the appropriate arm after target presentation, and we compared it with a condition in which the reaching arm was cued in advance. The two conditions effectively controlled for sensory input, spatial attention, and motor output and differed only with respect to the need to select the effector after target onset in the uncued condition. Results revealed that irrespective of cue condition, dmPPC and PMdc activity during the RT interval (i.e., after target presentation) was primarily observed contralateral to the reaching arm. Interestingly, the recruitment of these regions was significantly delayed in the uncued compared with the cued condition, with the difference in dmPPC latency predicting well the subjects' difference in RT across conditions. Together, these results demonstrate that effector selection is not associated with the simultaneous specification of motor goals tied to the two arms in bilateral dmPPC and PMdc, but rather suggest that a motor goal is formed in these regions only after an arm is selected for action.

The main finding of the present study relates to the change in the latency of activation in contralateral dmPPC and PMdc depending on whether arm selection had to be achieved or not. This delay was evident in the fMRI deconvolution analysis (Fig. 3*B*) and was confirmed with EEG (Figs. 5 and 6). The two connected regions thus appear to have acted downstream from the selection of the arm. One important implication of this result is that incoming (i.e., bottom-up) visuospatial signals are not "automatically" integrated with arm postural signals in dmPPC and PMdc to form a motor goal. Rather, this process appears to necessitate the presence of an internal signal related to the intention to use a particular arm. It is unclear exactly

how intention allows the target and arm signals to be bound into a motor goal in these regions, but the signature of this intentional drive may be the tonic preparatory activity that is observed in contralateral dmPPC (Beurze et al. 2007; Calton et al. 2002) and PMdc (Beurze et al. 2007; Hoshi and Tanji 2006) in response to the instruction to use a particular arm, before a visuospatial target is presented. In support of this idea, monkey work recently reported that the magnitude of this nonspatial preparatory firing in PRR was significantly correlated with reach RT of the contralateral limb (Snyder et al. 2006). Hence, the RT differences observed here across conditions are well predicted by differences in the timing of dmPPC recruitment (Fig. 6, *left*), which may be the consequence of the presence or absence of a cue-induced preparatory drive.

Two separate regions within the parietofrontal cortex showed greater activity in the uncued compared with the cued condition: the mIPS and PMdr. Importantly, these higher levels of activation were only observed ipsilateral to the reaching arm, consistent with the hypothesis that some level of planning of the "incorrect" arm may have been transiently elaborated in the uncued condition. Although both of these regions are involved in sensorimotor transformations, they are thought to play a relatively "early" role in the motor planning hierarchy. For instance, human mIPS has a retinotopic organization (Medendorp et al. 2003; Sereno et al. 2001) and uses gaze-centered encoding to represent spatial goal locations (Medendorp et al. 2003). In support of a more sensory role, we found that mIPS was active in a purely passive version of the present task in which subjects viewed the visual targets but did not plan a reach toward them (Fig. 4*B*). Similarly, PMdr is also thought to be mostly involved in spatial and cognitive aspects of action, largely due to its dense connections with the prefrontal cortex (Barbas and Pandya 1987; Luppino et al. 1993). Accordingly, PMdr cells are well tuned to visual target locations but less so to the arm being used when reaching (Hoshi and Tanji 2006). Interestingly, in monkeys this region has been shown to be the primary locus for competition at the level of goal selection, while more caudal PMdc encoded only the outcome of the decision (Cisek 2006; Cisek and Kalaska 2002). In this framework, mIPS and PMdr may have contributed to the active maintenance of the spatial coordinates of the goal (Cisek 2006; Curtis and D'Esposito 2006). When the effector was known in advance (cued condition), target visuospatial signals might have been specified predominantly in the hemisphere contralateral to the reaching arm. In contrast, in the uncued condition, given the uncertainty associated with the effector to be used, spatial goals might have been represented in bilateral mIPS and PMdr, in preparation for either arm being selected (Fig. 7). Once selection of the arm was achieved, these spatial signals might then have been relayed to PMdc and dmPPC contralateral to the reaching arm to be integrated with arm-related signals and generate a motor goal. Overall, such a division of labor between subregions of the parietofrontal cortex is supported by distinct connectivity patterns in monkeys, with area PEc (mIPS) being primarily connected to F7 (PMdr) and V6Ad (dmPPC) being connected primarily to F2 (PMdc) (Gamberini et al. 2009).

A set of other regions in the frontal lobe was more active in the uncued than in the cued condition (Fig. 3*C*). These include the anterior cingulate as well as BA 9 and BA 46, which make up the dorsolateral prefrontal cortex (dlPFC) (Petrides and

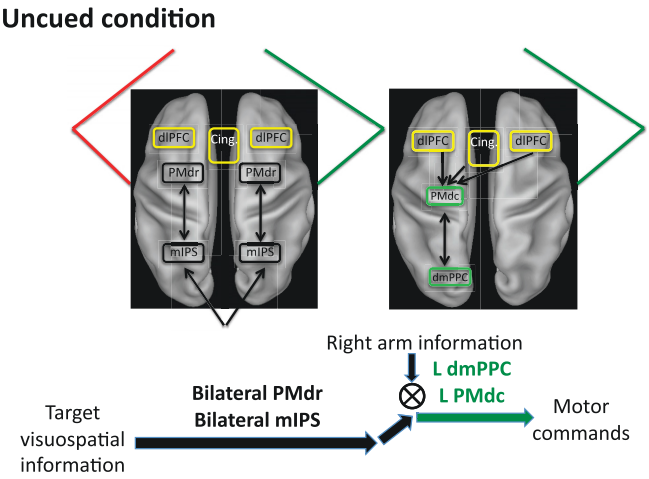

Fig. 7. Potential mechanism for effector selection. When the arm is not known in advance (uncued condition), target visuospatial signals are maintained in bilateral rostral dorsal premotor complex (PMdr) and mIPS, in preparation for either arm being selected for action. Upon selection of the appropriate arm based on the color of the target [in the dorsolateral prefrontal cortex (dlPFC) and anterior cingulate (Cing.)], the target sensory signals are integrated with the arm sensory signals to form a motor goal in contralateral PMdc and dmPPC.

Pandya 1999). These regions may have contributed to the cognitive process of selecting the arm based on the color of the target. The dlPFC is critical for linking information maintained in short-term memory to the organization of actions (Pochon et al. 2001), allowing for monitoring and updating of the status of intended acts (Petrides et al. 1995; Petrides and Pandya 1999). Through connections with premotor areas (Takada et al. 2004), the decision outcome (i.e., the intention to use a particular arm) may then have been fed back to the arm-selective regions of the parietofrontal cortex for a motor goal to be specified. In support of this, recent electrophysiological work in monkeys has revealed parietofrontal latency differences between PMd and PRR in a target-choice task (Pesaran et al. 2008) as well as in nonstandard visuomotor tasks such as anti-reaching (Westendorff et al. 2010). This front-to-back information flow is further supported by our finding that dmPPC timing better predicted the moment of reach onset than did PMdc (Fig. 6). Although these data do not speak to the functional interactions between these regions, the correlation between dmPPC timing and RT certainly suggests that this region played a role in the late executive stages of sensorimotor transformations.

Consistent with the present findings, a recent study argued that the process of effector selection occurs in a more serial manner than target selection. Using a task in which monkeys had to select an arm or an eye movement to achieve a target, Cui and Andersen (2011) showed that cells in parietal area 5d became significantly active only after the arm was unambiguously specified as the effector. This finding is qualitatively similar to our delay in dmPPC recruitment until after an arm was selected in the uncued condition. An interesting distinction between the results of the two studies is that we found the "bottleneck" to occur in the dmPPC, a region that is thought to be hierarchically upstream from area 5d (Cui and Andersen 2011). Although this different pattern of results may reflect neuroanatomic differences across species, it could also pertain to the type of decision to be made across the tasks [arm vs. eye movement in Cui and Andersen (2011); arm vs. arm movement in our study]. Specifically, in arm vs. eye selection tasks, there

may be a tendency to engage the networks of both effectors in parallel to a "deeper" extent (i.e., more downstream) given that they are often used jointly in the natural world. Conversely, the mutually exclusive nature of the selection of one arm among the two may render the recruitment of the arm-selective regions of the PPC dependent on prior selection of the arm.

The simultaneous specification of multiple potential goals is a ubiquitous phenomenon in the brain. Multiple reaching movements can coexist simultaneously in PMdr (Cisek and Kalaska 2002) and dmPPC (Klaes et al. 2011; Scherberger and Andersen 2007), multiple potential saccades can be specified in parallel in the superior colliculus (Basso and Wurtz 1997), and multiple grasps can be encoded in anterior IPS (Baumann et al. 2009). The present findings add to the current knowledge by placing a contingency on this framework. They suggest that, at least in the reach domain, effector selection is a prerequisite for a motor goal to be specified. Target goals are represented in an arm-independent manner in mIPS and PMdr until an arm is selected to act upon them, at which point these spatial signals are integrated with arm-related postural signals to form a motor goal in dmPPC and PMdc.

ACKNOWLEDGMENTS

We thank Shant Donoyan for help with data processing.

GRANTS

This work was supported by the Fonds Québécois de Recherche sur la Nature et les Technologies (to P. M. Bernier), National Institute of Neurological Disorders and Stroke Grant NS44393 (to S. T. Grafton), and the Institute for Collaborative Biotechnologies through U.S. Army Research Office Grant W911NF-09-0001 (to S. T. Grafton).

DISCLOSURES

No conflicts of interest, financial or otherwise, are declared by the authors.

AUTHOR CONTRIBUTIONS

Author contributions: P.-M.B. and S.T.G. conception and design of research; P.-M.B. performed experiments; P.-M.B. and M.C. analyzed data; P.-M.B. and S.T.G. interpreted results of experiments; P.-M.B. prepared figures; P.-M.B. drafted manuscript; P.-M.B. and S.T.G. edited and revised manuscript; P.-M.B. and S.T.G. approved final version of manuscript.

REFERENCES

Allen PJ, Josephs O, Turner R. A method for removing imaging artifact from continuous EEG recorded during functional MRI. *Neuroimage* 12: 230–239, 2000.

Allen PJ, Polizzi G, Krakow K, Fish DR, Lemieux L. Identification of EEG events in the MR scanner: the problem of pulse artifact and a method for its subtraction. *Neuroimage* 8: 229–239, 1998.

Andersen RA, Buneo CA. Intentional maps in posterior parietal cortex. *Annu Rev Neurosci* 25: 189–220, 2002.

Babiloni F, Cincotti F, Carducci F, Rossini PM, Babiloni C. Spatial enhancement of EEG data by surface Laplacian estimation: the use of magnetic resonance imaging-based head models. *Clin Neurophysiol* 112: 724–727, 2001.

Barbas H, Pandya DN. Architecture and frontal cortical connections of the premotor cortex (area 6) in the rhesus monkey. *J Comp Neurol* 256: 211–228, 1987.

Basso MA, Wurtz RH. Modulation of neuronal activity by target uncertainty. *Nature* 389: 66–69, 1997.

Baumann MA, Fluet MC, Scherberger H. Context-specific grasp movement representation in the macaque anterior intraparietal area. *J Neurosci* 29: 6436–6448, 2009.

Berg P, Scherg M. A fast method for forward computation of multiple-shell spherical head models. *Electroencephalogr Clin Neurophysiol* 90: 58–64, 1994.

Bernier PM, Grafton ST. Human posterior parietal cortex flexibly determines reference frames for reaching based on sensory context. *Neuron* 68: 776–788, 2010.

Beurze SM, de Lange FP, Toni I, Medendorp WP. Integration of target and effector information in the human brain during reach planning. *J Neurophysiol* 97: 188–199, 2007.

Buracas GT, Boynton GM. Efficient design of event-related fMRI experiments using M-sequences. *Neuroimage* 16: 801–813, 2002.

Calhoun VD, Stevens MC, Pearlson GD, Kiehl KA. fMRI analysis with the general linear model: removal of latency-induced amplitude bias by incorporation of hemodynamic derivative terms. *Neuroimage* 22: 252–257, 2004.

Calton JL, Dickinson AR, Snyder LH. Non-spatial, motor-specific activation in posterior parietal cortex. *Nat Neurosci* 5: 580–588, 2002.

Chang SW, Dickinson AR, Snyder LH. Limb-specific representation for reaching in the posterior parietal cortex. *J Neurosci* 28: 6128–6140, 2008.

Cisek P. Integrated neural processes for defining potential actions and deciding between them: a computational model. *J Neurosci* 26: 9761–9770, 2006.

Cisek P, Kalaska JF. Simultaneous encoding of multiple potential reach directions in dorsal premotor cortex. *J Neurophysiol* 87: 1149–1154, 2002.

Connolly JD, Andersen RA, Goodale MA. FMRI evidence for a 'parietal reach region' in the human brain. *Exp Brain Res* 153: 140–145, 2003.

Cui H, Andersen RA. Different representations of potential and selected motor plans by distinct parietal areas. *J Neurosci* 31: 18130–18136, 2011.

Cui H, Andersen RA. Posterior parietal cortex encodes autonomously selected motor plans. *Neuron* 56: 552–559, 2007.

Culham JC, Cavina-Pratesi C, Singhal A. The role of parietal cortex in visuomotor control: what have we learned from neuroimaging? *Neuropsychologia* 44: 2668–2684, 2006.

Curtis CE, D'Esposito M. Selection and maintenance of saccade goals in the human frontal eye fields. *J Neurophysiol* 95: 3923–3927, 2006.

Diedrichsen J, Shadmehr R. Detecting and adjusting for artifacts in fMRI time series data. *Neuroimage* 27: 624–634, 2005.

Fabbri S, Caramazza A, Lingnau A. Tuning curves for movement direction in the human visuomotor system. *J Neurosci* 30: 13488–13498, 2011.

Galletti C, Fattori P, Kutz DF, Battaglini PP. Arm movement-related neurons in the visual area V6A of the macaque superior parietal lobule. *Eur J Neurosci* 9: 410–413, 1997.

Gamberini M, Passarelli L, Fattori P, Zucchelli M, Bakola S, Luppino G, Galletti C. Cortical connections of the visuomotor parietooccipital area V6Ad of the macaque monkey. *J Comp Neurol* 513: 622–642, 2009.

Genovese CR, Lazar NA, Nichols T. Thresholding of statistical maps in functional neuroimaging using the false discovery rate. *Neuroimage* 15: 870–878, 2002.

Gratton G, Coles MG, Donchin E. A new method for off-line removal of ocular artifact. *Electroencephalogr Clin Neurophysiol* 55: 468–484, 1983.

Homan RW, Herman J, Purdy P. Cerebral location of international 10–20 system electrode placement. *Electroencephalogr Clin Neurophysiol* 66: 376–382, 1987.

Hoshi E, Tanji J. Differential involvement of neurons in the dorsal and ventral premotor cortex during processing of visual signals for action planning. *J Neurophysiol* 95: 3596–3616, 2006.

Klaes C, Westendorff S, Chakrabarti S, Gail A. Choosing goals, not rules: deciding among rule-based action plans. *Neuron* 70: 536–548, 2011.

Krams M, Rushworth MF, Deiber MP, Frackowiak RS, Passingham RE. The preparation, execution and suppression of copied movements in the human brain. *Exp Brain Res* 120: 386–398, 1998.

Lancaster JL, Rainey LH, Summerlin JL, Freitas CS, Fox PT, Evans AC, Toga AW, Mazziotta JC. Automated labeling of the human brain: a preliminary report on the development and evaluation of a forward-transform method. *Hum Brain Mapp* 5: 238–242, 1997.

Lancaster JL, Woldorff MG, Parsons LM, Liotti M, Freitas CS, Rainey L, Kochunov PV, Nickerson D, Mikiten SA, Fox PT. Automated Talairach atlas labels for functional brain mapping. *Hum Brain Mapp* 10: 120–131, 2000.

Lindquist MA, Meng Loh J, Atlas LY, Wager TD. Modeling the hemodynamic response function in fMRI: efficiency, bias and mis-modeling. *Neuroimage* 45: S187–S198, 2009.

Liu TT. Efficiency, power, and entropy in event-related fMRI with multiple trial types. Part II: design of experiments. *Neuroimage* 21: 401–413, 2004.

Luppino G, Matelli M, Camarda R, Rizzolatti G. Corticocortical connections of area F3 (SMA-proper) and area F6 (pre-SMA) in the macaque monkey. *J Comp Neurol* 338: 114–140, 1993.

Manahilov V, Riemslag FC, Spekreijse H. The Laplacian analysis of the pattern onset response in man. *Electroencephalogr Clin Neurophysiol* 82: 220–224, 1992.

Medendorp WP, Goltz HC, Vilis T, Crawford JD. Gaze-centered updating of visual space in human parietal cortex. *J Neurosci* 23: 6209–6214, 2003.

Perrin F, Bertrand O, Pernier J. Scalp current density mapping: value and estimation from potential data. *IEEE Trans Biomed Eng* 34: 283–288, 1987.

Pesaran B, Nelson MJ, Andersen RA. Free choice activates a decision circuit between frontal and parietal cortex. *Nature* 453: 406–409, 2008.

Petrides M, Alivisatos B, Evans AC. Functional activation of the human ventrolateral frontal cortex during mnemonic retrieval of verbal information. *Proc Natl Acad Sci USA* 92: 5803–5807, 1995.

Petrides M, Pandya DN. Dorsolateral prefrontal cortex: comparative cytoarchitectonic analysis in the human and the macaque brain and corticocortical connection patterns. *Eur J Neurosci* 11: 1011–1036, 1999.

Pochon JB, Levy R, Poline JB, Crozier S, Lehericy S, Pillon B, Deweer B, Le Bihan D, Dubois B. The role of dorsolateral prefrontal cortex in the preparation of forthcoming actions: an fMRI study. *Cereb Cortex* 11: 260–266, 2001.

Rushworth MF, Krams M, Passingham RE. The attentional role of the left parietal cortex: the distinct lateralization and localization of motor attention in the human brain. *J Cogn Neurosci* 13: 698–710, 2001.

Scherberger H, Andersen RA. Target selection signals for arm reaching in the posterior parietal cortex. *J Neurosci* 27: 2001–2012, 2007.

Sereno MI, Pitzalis S, Martinez A. Mapping of contralateral space in retinotopic coordinates by a parietal cortical area in humans. *Science* 294: 1350–1354, 2001.

Snyder LH, Batista AP, Andersen RA. Coding of intention in the posterior parietal cortex. *Nature* 386: 167–170, 1997.

Snyder LH, Dickinson AR, Calton JL. Preparatory delay activity in the monkey parietal reach region predicts reach reaction times. *J Neurosci* 26: 10091–10099, 2006.

Takada M, Nambu A, Hatanaka N, Tachibana Y, Miyachi S, Taira M, Inase M. Organization of prefrontal outflow toward frontal motor-related areas in macaque monkeys. *Eur J Neurosci* 19: 3328–3342, 2004.

Van Essen DC. A Population-Average, Landmark- and Surface-based (PALS) atlas of human cerebral cortex. *Neuroimage* 28: 635–662, 2005.

Westendorff S, Klaes C, Gail A. The cortical timeline for deciding on reach motor goals. *J Neurosci* 30: 5426–5436, 2010.